Sparse Representation for Signal Reconstruction in Calorimeters Operating in High Luminosity

Davis P. Barbosa, Luciano M. de A. Filho, Bernardo S. Peralva, Augusto S. Cerqueira, and José M. de Seixas

***Abstract*— A calorimeter signal reconstruction method, based on sparse representation (SR) of redundant data, is proposed for energy reconstruction in particle colliders operating in high-luminosity conditions. The signal overlapping is first modeled as an underdetermined linear system, leading to a convex set of feasible solutions. The solution with the smallest number of superimposed signals (the SR) that represents the recorded data is obtained through the use of an interior-point (IP) optimization procedure. From a signal processing point-of-view, the procedure performs a source separation, where the information of the amplitude of each convoluted signal is obtained. In the simulation results, a comparison of the proposed method with standard signal reconstruction one was performed. For this, a toy Monte Carlo simulation was developed, focusing in calorimeter front-end signal generation only, where the different levels of pileup and signal-to-noise ratio were used to qualify the proposed method. The results show that the method may be competitive in high-luminosity environments.**

***Index Terms*— Amplitude estimation, calorimetry, high-luminosity colliders, optimal filters (OFs), sparse representation (SR).**

I. Introduction

CALORIMETERS are indispensable apparatus in high-energy physics experiments [1]. Typically, they are segmented into layers and comprise thousands of readout channels from which the energy of incoming particles is sampled and estimated. Classical energy reconstruction methods are based on the stability of a conditioned pulse shape whose amplitude is proportional to the energy of the incident particles [2]. However, for calorimeters operating in high-event rate particle colliders (tens of MHz) [3], [4], and high luminosity, the signal overlapping (pileup) degrades the final energy reconstruction [5]. Standard techniques interpret these superimposed signals as noise from which the second-order statistics is extracted to develop a linear optimal filter (OF). The OF aims at minimizing the pileup contribution on the estimation of the central signal amplitude [5]–[7].

The interpretation of the pileup as noise, as performed by OF, presents some drawbacks: 1) OF design becomes luminosity-dependent; 2) noise distribution is no longer Gaussian and hence the linear filter operates in suboptimal conditions; and 3) extra information provided by the adjacent signals is discarded.

An alternative algorithm, which is based on a deconvolution processing approach, has recently been proposed [8] and treats the pileup properly as superimposed signals, designing an orthogonal vector amplitude estimator from which the amplitudes of all detected superimposed signals are estimated simultaneously. The orthogonality constraint improves the energy reconstruction performance under pileup, recovering the noise Gaussian behavior. Furthermore, it provides a design that is luminosity-independent and gives additional information about the energy from signals at adjacent bunch-crossings (BCs).

The whole deconvolution technique, as proposed in [8], implements a two-step algorithm. The first step is a procedure for pileup identification, which is performed through a deconvolution matrix (DM). A threshold is applied at the DM outputs in order to identify which BCs have high-energy signal contribution. The second step performs a vector amplitude estimation procedure, where only signals identified at the first step are taken into account. Therefore, while the first step indicates where the signals with relevant information are, the second estimates their amplitudes with high accuracy, since a minimal number of orthogonality constraints are applied.

DM works properly for signals that fit within the acquired window, which is the case for most of the current calorimeters operating in high-luminosity colliders [7], [9]–[12]. As a result, in this condition, pulses outside the window produce small contributions on the central signal amplitude estimation. However, in calorimeter cells that are located at regions of very high signal occupancy, DM starts to decrease in performance [8] due to the presence of signal tails that were not taken into account. This is particularly important in designs using bipolar shaping front-end electronics and restricting the reconstruction process to samples of the positive lobule [13], [14]. Therefore, in order to increase the performance of the deconvolution method in these special conditions, a new preprocessing method for pileup identification is proposed here.

The proposed method consists of finding a suitable solution for an underdetermined system of equations. Classical procedures for this task, like least square (LS) and χ^2 methods [15], rely on the minimization of the Euclidean norm. However, this approach tends to spread the information among the adjacent BCs. From a calorimeter energy reconstruction perspective, this leakage effect provokes underestimation of the actual energy values, at the same time that produces false alarm

Manuscript received April 6, 2017; accepted May 31, 2017. Date of publication June 6, 2017; date of current version July 14, 2017. This work was supported in part by CAPES, in part by CNPq, in part by FAPERJ, in part by FAPEMIG, and in part by the National Network for High Energy Physics (RENAFAE) in Brazil.

D. P. Barbosa, L. M. A. Filho, and A. S. Cerqueira are with the Electrical Engineering Department, Federal University of Juiz de Fora, Juiz de Fora 36036-900, Brazil (e-mail: luciano.manhaes.de.andrade.filho@cern.ch).

B. S. Peralva is with the Computational Modeling Department, Rio de Janeiro State University, Nova Friburgo 28625-570, Brazil.

J. M. de Seixas is with the Electrical Engineering Department, Federal University of Rio de Janeiro, Rio de Janeiro 21945-970, Brazil.

Digital Object Identifier 10.1109/TNS.2017.2712420

in BCs near to the ones with relevant information. Based on this rationale, instead of minimizing a squared cost function, we propose to look for the solution that concentrates the information in few components, avoiding the leakage effect to neighborhood BCs. This decomposition may be performed using modern sparse representation (SR) of data [16].

SR stands for a signal decomposition, where the new representation of the data present the smallest number of nonzero components [17]. SR for underdetermined systems of equations is a core engine in many signal processing developments, such as data compression, source separation, and deconvolution procedures [18]. Today, several competitive algorithms are available [19], [20]. One of the most efficient algorithms for SR relies on the well-established linear programming (LP) theory [21]. In this paper, we implement the SR method based on LP, but a modification is proposed, in order to promote positive amplitude solutions, as required in calorimetry.

In order to quantify the efficiency of the proposed method and to better understand in which conditions it suits best, we compare the performance of the deconvolution methods using SR and DM as preprocessing step. This is evaluated through a toy Monte Carlo simulation, similar to the one presented in [8], adding a situation where the reference pulse shape may not completely fit into the acquisition window, which is often the case for the acquisition of only the positive lobule of bipolar pulses [14]. For sake of completeness, results with a standard OF design are also included. The toy Monte Carlo simulation focuses in the front-end signal generation only, allowing the synthetic generation of different calorimeter pulse shapes and different levels of pileup and signal-to-noise ratio. The main advantage of this simulation is the flexibility, while the main drawback is its limited scope.

This paper is organized as follows. Section II describes the OF technique and the deconvolution method using DM. Section III presents the SR method based on LP. Section IV treats the implementation of the SR algorithm aiming at pileup detection in sampling calorimeters. In Section V, the simulation set is presented and the proposed method is compared with other energy estimation methods. Finally, the conclusions are derived in Section VI.

II. Energy Reconstruction Methods

A. Optimal Filter Algorithm

The OF method describes the calorimeter signal as a first-order approximation [5]

$$\mathbf{r} = A\mathbf{h} - A\tau\dot{\mathbf{h}} + \mathbf{w} \tag{1}$$

where $\mathbf{r}$ corresponds to the calorimeter time sample vector and the amplitude A is the parameter to be estimated, while $\mathbf{w}$ is the additive noise. The vectors $\mathbf{h}$ and $\dot{\mathbf{h}}$ are, respectively, the calorimeter response (time samples) and its derivative (linear approximation for the pulse phase), while the parameter τ is the signal phase.

In the absence of signal pileup condition, the noise comprises mainly electronic noise, which is often assumed stationary and modeled by a Gaussian distribution. Therefore, a variance minimization technique may be applied to recover the parameter of interest as it performs close to the optimal operation. The OF algorithm relies on such condition to develop a linear estimator based on a weighted sum operation, where the signal amplitude A is recovered through

$$\hat{A} = \mathbf{g}'\mathbf{r}. \tag{2}$$

The weights $\mathbf{g}$ are obtained from the front-end pulse shape and the noise covariance matrix. The prime symbol denotes the transpose operation. Since the OF procedure aims at computing the correct set of weights that minimize the effect of the noise, its design leads to the optimum estimator for deterministic signals corrupted from Gaussian noise.

For a linear and unbiased estimator, it is required that the expected value of $\hat{A}$ to be A. Additionally, by assuming the noise as a zero-mean random process ($E[w] = 0$), it results in

$$E[\hat{A}] = (A\mathbf{g}'\mathbf{h} - A\tau\mathbf{g}'\dot{\mathbf{h}}). \tag{3}$$

As a result, the following two constraints can be deduced and added to the minimization procedure in order to reach the condition $E[\hat{A}] = A$:

$$\mathbf{g}'\mathbf{h} = 1 \tag{4}$$

$$\mathbf{g}'\dot{\mathbf{h}} = 0. \tag{5}$$

The variance of a linear estimator is given by [15]

$$\mathrm{var}(\hat{A}_{\mathrm{OF}}) = \mathbf{g}'\mathbf{C}\mathbf{g} \tag{6}$$

where $\mathbf{C}$ corresponds to the noise covariance matrix and $\mathbf{g}$ is the weighting vector. Hence, to find the optimal weights, (6) is often minimized subjected to the constraints in (4) and (5) using Lagrange multipliers [5].

It should be stressed that, in high-luminosity conditions, the noise covariance matrix absorbs the information from the signal pileup second-order statistics. However, since the superimposed pulses introduce higher order statistics to the noise (non-Gaussian distribution), the information from the covariance matrix is not enough to properly describe the noise. As a result, the OF design may lead to a suboptimal design in such conditions.

B. Deconvolution Approach

The deconvolution method was originally proposed to deal with calorimeter signal reconstruction in high-luminosity environments, where the full signal fits within the readout window.

Unlike the OF design, the deconvolution method designs an orthogonal estimating vector, represented by a $\mathbf{G}_p$ coefficient matrix, aiming at estimating the amplitudes of p predetected overlapped signals

$$\hat{\mathbf{a}}_p = \mathbf{G}_p'\mathbf{r} \tag{7}$$

where $\hat{\mathbf{a}}_p$ is the estimated amplitude vector. Providing that the BC indices of the superimposed signals are known in advance, the method designs orthogonal estimators for the predetected overlapped signals. Given an $\mathbf{H}_p$ matrix, whose columns are formed from the reference pulse shapes of p superposed signals (shifted version of the calorimeter pulse shape), the coefficients of the $\mathbf{G}_p$ matrix can be determined as

$$\mathbf{G}_p = \mathbf{H}_p\left(\mathbf{H}_p'\mathbf{H}_p\right)^{-1}. \tag{8}$$

Equation (8), which is valid for white Gaussian noise [8], states that the amplitudes of the superimposed signals can be estimated simultaneously, providing that the BC indices for the overlapped signals are known in advance.

For signals that fit within the acquisition window, the preprocessing for pileup identification can be performed using (8) as well [8]. However, at this step, it is assumed the presence of signals in all BCs within the window. This is performed through a squared $\mathbf{H}_s$ matrix, simplifying (8) as

$$\mathbf{G}_s = \mathbf{H}_s^{-1}. \tag{9}$$

The $\mathbf{H}_s^{-1}$ matrix is the DM. Thus, for a window of W recorded samples, DM is able to estimate the amplitude of the signals for W adjacent BCs. After DM computation, a threshold is applied to each estimate, in order to detect which BC has relevant pileup contribution.

As the DM preprocessing is performed on samples within the acquisition window, it may operate with lower performance for signals, whose samples are not fully acquired [8].

III. Sparse Representation

We start with the problem of solving an underdetermine system of equations

$$\mathbf{r} = \mathbf{H}\mathbf{a} \tag{10}$$

where $\mathbf{r}$ is a known vector of W variables, $\mathbf{H}$ is a known matrix of dimension $W \times M$, and $\mathbf{a}$ is an unknown vector of dimension M. For the case, where $M > W$, the system has infinite solutions for the vector $\mathbf{a}$. Thus, one must determine an objective function in order to define a criterium for selecting the most suitable solution. A common approach in signal processing is to select the $\mathbf{a}$ vector with the smallest Euclidean norm squared $\|\mathbf{a}\|_2^2$, defined here as the l_2-norm. This rule defines the optimization problem

$$\min_{\mathbf{a}} \|\mathbf{a}\|_2^2 \quad \text{s.t. } \mathbf{r} = \mathbf{H}\mathbf{a} \tag{11}$$

leading to a strictly convex problem with a unique solution known as the LS solution [16]

$$\mathbf{a} = \mathbf{H}'(\mathbf{H}\mathbf{H}')^{-1}\mathbf{r}. \tag{12}$$

LS is largely used in stochastic signal processing due to the simplicity of the corresponding design and the strong correlation with Wiener and Kalman filters [22]. In order to minimize the Euclidean norm, LS populates several components of the $\mathbf{a}$ vector with small amplitudes and both positive and negative values.

Next, we derive an objective function that concentrates the sources in few positive amplitude signals, which better represent the deconvolution of positive amplitude signals. This procedure is equivalent of finding the sparsest representation of the data.

A. Objective Function for Sparse Representation

Stating a generic l_q-norm problem

$$\min_{\mathbf{a}} \|\mathbf{a}\|_q^q \quad \text{s.t. } \mathbf{r} = \mathbf{H}\mathbf{a} \tag{13}$$

where

$$\|\mathbf{a}\|_q^q = \sum_{i=1}^{M} |a_i|^q \tag{14}$$

it can be shown [16] that the smaller the q-value, more sparse tends to be the solution and the sparsest one is found in the limit for $q \to 0$. However, for $q < 1$, the problem in (13) is no longer convex and it is not tractable with regular optimization theory. Thus, for practical implementations, the sparsest solution for $\mathbf{a}$ in (10) is approximated using the l_1-norm in (13).

A direct minimization of the l_1-norm is not possible due to the discontinuity present at the origin on this equation. However, this discontinuity can be avoided splitting the $\mathbf{a}$ vector into two vectors $\mathbf{u}$ and $\mathbf{v}$, containing the positive and negative elements of $\mathbf{a}$, respectively. Thus, without the loss of generalization, the problem in (13), for $q = 1$, can be modified as follows: let $\mathbf{a}$ be defined as a combination of two vectors of the form $\mathbf{a} = \mathbf{u} - \mathbf{v}$ and concatenating $\mathbf{u}$ and $\mathbf{v}$ in a vector $\mathbf{z}$ of size $2M$, comprising only nonnegative elements, the linear model in (10) is restated as

$$\mathbf{r} = \mathbf{H}^{\dagger}\mathbf{z} \tag{15}$$

where $\mathbf{H}^{\dagger} = [\mathbf{H} - \mathbf{H}]$ is the concatenation of the $\mathbf{H}$ and $-\mathbf{H}$ matrices. The l_1-norm minimization problem can be rewritten according to

$$\min_{\mathbf{z}} \mathbf{1}'\mathbf{z} \quad \text{s.t.} \begin{cases} \mathbf{r} = \mathbf{H}^{\dagger}\mathbf{z} \\ \mathbf{z} \geq \mathbf{0} \end{cases} \tag{16}$$

where $\mathbf{1}$ represents a vector with all the elements equal to unity. This optimization problem stands for a linear objective function with linear (equality and inequality) constraints. This problem follows a regular LP optimization procedure, whose solution can be obtained using several classes of well-established algorithms. The implemented routine is based on [23], which is a variant of the predictor–corrector algorithm proposed in [24], a primal-dual IP method [25].

B. Sparse Representation Under Noise

In a more realistic signal processing problem, the vector $\mathbf{r}$ in (10) is embedded in additive noise. In this case, the linear model yields

$$\mathbf{r} = \mathbf{H}\mathbf{a} + \mathbf{w} \tag{17}$$

where $\mathbf{w}$ is a zero-mean noise vector.

In such conditions, the equality constraint in (16) can be relaxed, allowing a small deviation $\mathbf{e}$ from the ideal solution

$$-\mathbf{e} < \mathbf{H}^{\dagger}\mathbf{z} - \mathbf{r} < \mathbf{e}. \tag{18}$$

This is not an issue for LP, since it works also with inequality constraints. In order to allow a different deviation to each recovered component in $\mathbf{a}$, the residual $\mathbf{H}^{\dagger}\mathbf{z} - \mathbf{r}$ can be projected onto the $\mathbf{H}$ matrix without the loss of generalization

$$-\mathbf{e} < \mathbf{H}'(\mathbf{H}^{\dagger}\mathbf{z} - \mathbf{r}) < \mathbf{e} \tag{19}$$

or

$$\mathbf{H}'\mathbf{r} - \mathbf{e} < \mathbf{H}'\mathbf{H}^{\dagger}\mathbf{z} < \mathbf{H}'\mathbf{r} + \mathbf{e}. \tag{20}$$

Notice that, in accordance to this transformation, now the $\mathbf{e}$ vector has dimension M instead of W. The optimal value for

the residual deviation **e** is found experimentally according to the noise source. From a calorimeter point-of-view, several noise sources, such as readout electronics, low amplitude pileup signals and crosstalk, deviation from the reference pulse shape, and so on, can be taken into account using this simple modification.

IV. SR Algorithm for Pileup Identification

As proposed in [8], the linear model of (10) can be used to represent the convolution equation [26]

$$r[n] = h[n] * a[n] \tag{21}$$

when W samples of the calorimeter output (represented by **r**) are available. For a system impulse response $h[n]$ covering N samples, the **a** vector has dimension $M = W + N - 1$ in order to cover all possible superposition patterns, and the **H** matrix contains those pattern vectors, which are shifted versions of the reference pulse.

In the DM case, the outer patterns (signal samples) of this **H** matrix are ignored, obtaining a square $\mathbf{H}_s$ matrix $W \times W$, and the amplitudes for the W central BC signals can be easily determined through the inversion of $\mathbf{H}_s$. In this paper, the complete solution for the M superimposed signals, represented by (17), is proposed using SR, extending the deconvolution process also to environments, where the entire signal is not acquired.

First, we compare the usage of the objective functions in (11) and (16) for finding a suitable solution for (10) in a deconvolution process. Fig. 1(a) shows the superposition of two shifted bipolar signals, representing a pileup of signals located at two different BCs. The bipolar signal was obtained from a typical *RC–CR* shaper circuitry often used in calorimetry [27]. Both original and the resulting overlapped signals are shown, together with five samples (the **r** vector), which are, here, considered for the reconstruction. Although the complete signal would cover $N = 21$ samples, for the chosen sample rate (40 MHz), only the samples located at the positive lobule of the central signal are used ($W = 5$).

In Fig. 1(b), the **a** vector components ($M = 21 + 5 - 1 = 25$), as recovered from both the LS [see (12)] and the noiseless SR [see (16)] methods are shown. Both methods use the same $\mathbf{H}_{5\times 25}$ matrix comprising all shifted versions of the reference pulse shape. The 25 components of **a** are indexed from -18 to 6 in order to highlight the position of the central signal (index $= 0$). The LS solution tends to spread the energy among adjacent components with small positive and negative amplitudes, since it aims at minimizing the overall Euclidean norm, which produces wrong source signal recovering. Supposing that a valid reconstruction is considered only at BC with positive amplitude values, the LS algorithm detects five superimposed signals from BC $= -1$ to 3. Although the LS algorithm is able to select the two BC with energy deposition (they are among the BCs with positive reconstructed amplitudes), it would under-estimate the actual energy values and generate three false-alarms for the second-deconvolution iteration.

On the other hand, due to the sparse configuration of the source, the proposed method correctly recovers the overlapped signal pattern, as shown by the full circles of Fig. 1(b), where the amplitude for the signals at BC $= 0$ and BC $= +2$ are correctly reproduced. This noiseless example illustrates the superior performance of using an objective function that promotes sparsity in the deconvolution process. The final algorithm is based on the noisy version given by (20) and also introduces *a priori* knowledge that the recovered energy values must be positive.

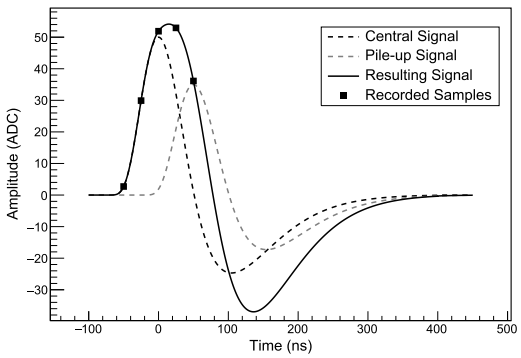

(a)

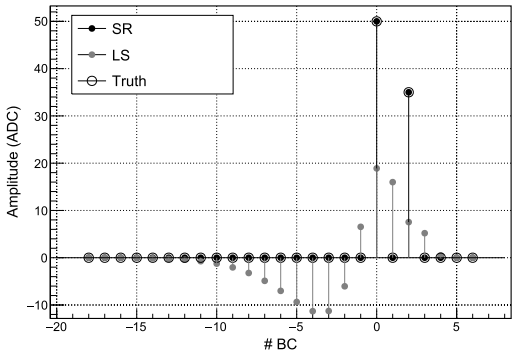

(b)

Fig. 1. Example of using SR for amplitude estimation. (a) Example of pileup due to signals at two different BCs. (b) Source recovering using LS and SR. Truth and SR information are superimposed, since the SR algorithm recovers the source without error, in this example.

A. Proposed Algorithm

In calorimetry, the acquired signal must sample a certain energy that is positive. Therefore, the vector of amplitudes **a** should store positive values only. Hence, we suggest a modification in the algorithm described in Section III in order to give a higher priority to positive amplitude reconstructions. This can be done by introducing a heavier weight k for the components of the **v** vector in the objective function, with respect to the **u** components. Thus, the proposed LP procedure for finding the pileup configuration in the preprocessing routine for deconvolution is

$$\min_{\mathbf{z}} (1-k)\mathbf{1}'\mathbf{u} + k\mathbf{1}'\mathbf{v} \quad \text{s.t.} \begin{cases} \mathbf{H}'\mathbf{r} - \mathbf{e} < \mathbf{H}'\mathbf{H}^{\dagger}\mathbf{z} < \mathbf{H}'\mathbf{r} + \mathbf{e} \\ \mathbf{z} \geq \mathbf{0} \\ 0 < k < 1. \end{cases} \tag{22}$$

The implemented algorithm uses the same primal-dual IP method used in the noiseless example earlier. The suitable values for both k and $\mathbf{e}$ are obtained through simulation.

V. Simulation Results

In this section, the proposed method is evaluated thorough a toy Monte Carlo simulation that focuses in the front-end signal generation only. The simulation is detailed, described, and the performance of the proposed method is compared with the OF and DM methods.

A. Simulation

In order to evaluate the performance of the proposed method, a computer-based setup was built to simulate a calorimeter signal digitization chain for a single cell. First, a raw data set comprising one million time samples, which represent a sequence of consecutive analog-to-digital converter samples from a general-purpose calorimeter output channel, is populated randomly with a given occupancy factor. At an extreme, 0% of occupancy means that no particle reaches the calorimeter cell. At the other extreme, an occupancy of 100% means that at every BC there is an impulse signal corresponding to a deposited energy. For the nonempty BC, an exponential distribution with mean value $\mu_{\text{pileup}} = 80$ MeV was used in order to emulate the energy deposition. Those are typical values of energy from pileup noise present, for instance, in the main LHC experiments [28], [29], which suffer a lot from the pileup problem. Centered at those BCs, reference pulse shape signals, with the respective amplitudes, are then superimposed, generating the pileup noise effect.

Two different pulses from an *RC–CR* shaping circuit were tested, depending on the R and C component parameters: a bipolar one, covering 500 ns and sampled at 40 MHz, and 200-ns width unipolar pulse sampled at 60 MHz, simulating different calorimeters operating at different high-event rate colliders. On both cases, the sampling rate is equal to the BC rate. Fig. 2 shows these reference signals. Before signal superposition, a pulse deformation is applied to each sample, using a normal distribution with $\sigma = 1\%$ of the sample value. Also, a random phase shift with an uniform distribution between $[-1, +1]$ ns simulates different time-of-flights for particles. After this step, a Gaussian white noise of 20 MeV [28] is added to each sample, simulating the electronic noise from the readout chain.

Next, the raw data set is split into windows of W samples, representing the pileup noise. Furthermore, the data set was equally divided in two: the development set ($\mathbf{D}$, a $W \times N_d$ matrix), which is used for the design of the estimation methods; and the test set ($\mathbf{T}$, a $W \times N_t$ matrix), from which estimation performance evaluation is assessed. For the unipolar pulse, $W = 12$ samples and $N_d = N_t = 41\,666$ events. For the bipolar pulse $W = 5$ samples and $N_d = N_t = 100\,000$ events. The development set is used to obtain the parameters required by the estimation methods. The OF method requires the noise covariance matrix, while the SR-COF requires the parameters (k, e). In order to evaluate the performance, the test set is used, assuring the generalization capability of the parameters obtained using the development set. Therefore, it is worth to mention that all results shown in this paper were generated using the test set.

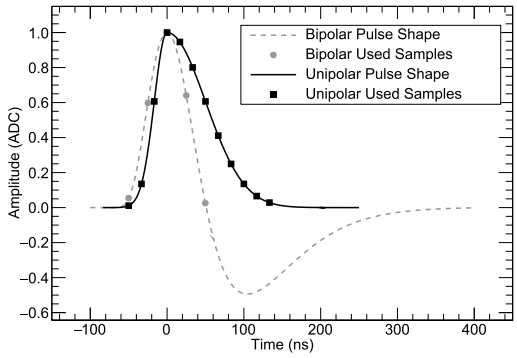

Fig. 2. Reference pulse shape for both unipolar and bipolar signals used in the simulation. The central signal samples ($W = 5$ and 12 for bipolar and unipolar, respectively) are also highlighted.

A central signal is added (including deformation and phase shift random distributions) in the test set, corresponding to the target signal, whose amplitude must be estimated. For these signals, the amplitude follows an exponential distribution with a given μ_{signal}, corresponding to different signal to pileup noise ratios (SPRs). The SPR is defined according to the following equation:

$$\text{SPR} = \frac{\mu_{\text{signal}}}{\mu_{\text{pileup}}} \tag{23}$$

where μ_{signal} and μ_{pileup} are mean values of the exponential distribution of the central signal and pileup amplitudes in the simulation, respectively.

B. Design of the Estimation Methods

The robust relative rms error (E_{rms}) between the truth (A) from the simulation (development set) and the reconstructed values ($\hat{A}$) was used as the criterium to select the best (k, e) set of parameters for the proposed method

$$E_{\text{rms}} = \sqrt{\frac{1}{N_s}\sum_{i=0}^{N_s-1}\left(\frac{\hat{A}_i - A_i}{A_i}\right)^2} \tag{24}$$

where N_s is the number of events selected by FAST-MCD algorithm [30] to avoid outliers.

The empirical procedure consists of ranging the values of those two parameters in a given range and selecting the values that reach the minimum of rms error surface. Therefore, (k, e) are chosen envisaging the minimization of the energy of the relative estimation error squared. As expected, only one set of parameters was selected for the proposed method, regardless the SPR and occupancy values used in the simulation: $k = 0.9$ and $k = 0.5$ for bipolar and unipolar pulses, respectively, and $\mathbf{e} = [0.12\ 0.12\ \cdots\ 0.12]$ [see (22)]. It should be stressed that k is computed according to the calorimeter pulse shape only, while the residual vector $\mathbf{e}$ is estimated from the calorimeter noise sources. Therefore, both k and $\mathbf{e}$ parameters are expected to be independent of the SPR and occupancy levels. Additionally, as the noise distribution of the digitized samples should be identically distributed, the elements of $\mathbf{e}$ are identical.

TABLE I

RELATIVE ENERGY ESTIMATION ERROR FOR DM AS A FUNCTION OF THE FRACTION OF SAMPLES USED FOR RECONSTRUCTION, CONSIDERING THE UNIPOLAR PULSE (20% OF OCCUPANCY AND SPR = 2)

Fraction of samples (%)	Relative Error (%)
50	294
58	200
67	159
75	163
83	125
92	138

Concerning the design of the OF method, a subset of development set ($\mathbf{D}_S$) [30] is used to compute the robust noise covariance matrix $\hat{\mathbf{C}}$, as the noise density distribution function is not known *a priori*

$$\hat{\mathbf{C}} = (\mathbf{D}_S - \overline{\mathbf{D}}_S)(\mathbf{D}_S - \overline{\mathbf{D}}_S)^T \tag{25}$$

where $\overline{\mathbf{D}}_S$ is defined as a $W \times N_s$ matrix, where all columns are equal to the vector that is the average over the N_s columns of the subset of the development set $\mathbf{D}_S$. It is worth to mention that $\hat{\mathbf{C}}$ must be calculated for each occupancy and SPR level.

C. Results

As previously mentioned, the acquisition window length (W) impacts on the DM performance. This is evaluated on the test set through the robust relative rms error (E_{rms}). Table I shows the percentage of the relative estimation error as a function of the fraction of samples (the acquisition window starts always at the first sample of the reference pulse used for reconstruction) considering the unipolar pulse and occupancy of 20%, SPR = 2 (typical pileup condition for triggered events). The percentage of the relative estimation error is the resulting error divided by error obtained when 100% of the samples are used for reconstruction. It can be seen that using 58% of the samples (7 of 12 samples) for reconstruction, the estimation error reaches twice the value of the full acquisition.

The deconvolution algorithms using SR (DEC-SR) and DM (DEC-DM) as preprocessing and the OF method were applied to the test set in order to reconstruct the amplitude of the central signal. Fig. 3 shows the relative error distribution for the reconstruction methods, for an occupancy level of 20% and SPR = 2. The summary of the robust rms and mean values for both unipolar and bipolar cases is shown in Table II. As expected, for the unipolar pulse, the performance is similar for both the deconvolution methods, while the OF performance is considerably worse. For the bipolar pulse, a better performance is observed for DEC-SR, while OF and DEC-DM performances are similar, as it can be seen from the error distribution profiles.

In order to quantify the performance of the algorithms for increasing pileup effect (in terms of occupancy and SPR values), simulations with different levels of occupancy and SPR were performed, following the same procedure described in Section V-A. Fig. 4 shows the robust relative rms error (24) for a fixed SPR = 2. For the unipolar pulse, both deconvolution methods present similar behavior and outperform OF, as expected. The OF performance

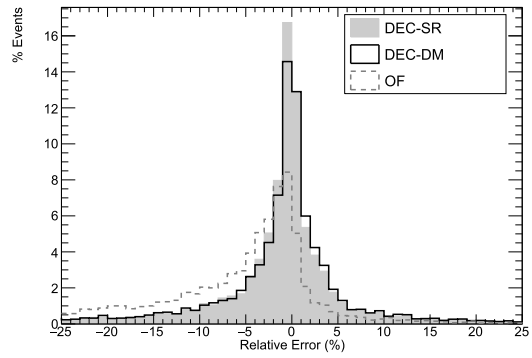

(a)

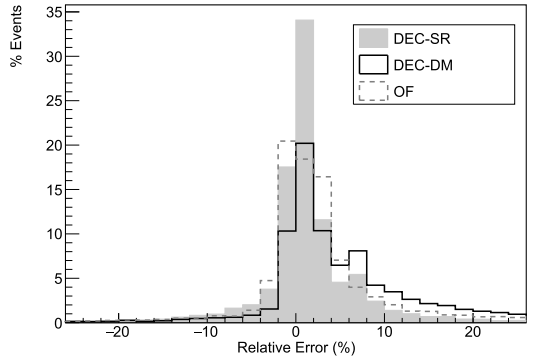

(b)

Fig. 3. Relative error for a run with 20% of occupancy and SPR = 2. (a) Unipolar pulse. (b) Bipolar pulse.

TABLE II

RMS AND MEAN VALUES OF THE RELATIVE ERRORS DISTRIBUTIONS FOR UNIPOLAR AND BIPOLAR PULSE RECONSTRUCTION

Type of pulse	Method	RMS values (%)	Mean values (%)
Unipolar	DEC-SR	4.17 ± 0.01	-1.05 ± 0.02
	DEC-DM	4.72 ± 0.02	-1.85 ± 0.02
	OF	13.37 ± 0.04	-8.32 ± 0.05
Bipolar	DEC-SR	2.687 ± 0.006	1.252 ± 0.007
	DEC-DM	8.65 ± 0.02	4.46 ± 0.02
	OF	7.35 ± 0.02	2.48 ± 0.02

collapses for high occupancy levels (above 10%). For the bipolar pulse, DEC-SR presents a better performance. Starting from 1% occupancy level, OF error increases significantly. Below the 1% occupancy level, DEC-DM and DEC-SR exhibit similar performance, but above this occupancy level, the use of SR as preprocessing for deconvolution is indicated, since the DM performance deteriorates. The DEC-SR performance stabilizes above 10% of occupancy.

The robust relative rms error as a function of the SPR is shown in Fig. 5 for the bipolar pulse, when an occupancy of 10% is fixed. As expected, the proposed technique (DEC-SR) presents better performance in regions of small SPR ratio, i.e., regions where the energy of the pileup signals is significant with respect to the energy of central signal. For higher SPR levels (>8) all methods present similar performance.

It is worth to mention that the algorithms exercised in the reported examples should be quantitatively evaluated in a

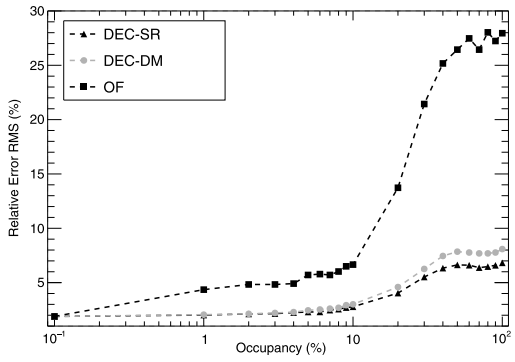

(a)

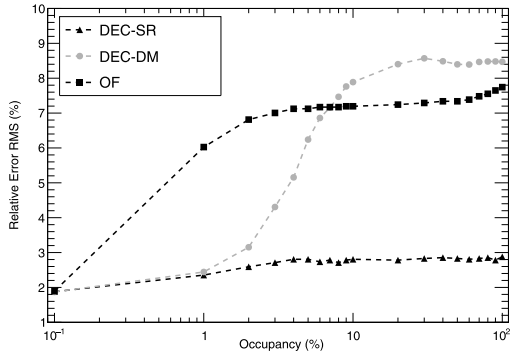

(b)

Fig. 4. Robust rms values of the relative error distributions as a function of the occupancy for SPR = 2. The error bars are small and cannot be seen. (a) Unipolar pulse. (b) Bipolar pulse.

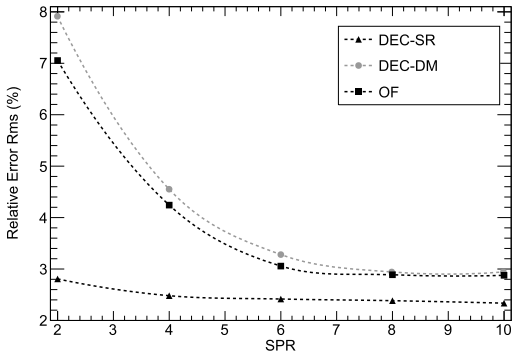

Fig. 5. Robust rms values of the relative error distributions as a function of the SPR for a fixed 10% occupancy (bipolar signal). The error bars are small and cannot be seen.

realistic experimental environment to achieve sound conclusions regarding their performance in real-life operation.

VI. Conclusion

The use of deconvolution for energy reconstruction has been expanded for considering signals that do not entirely fit within the acquisition window, which is often the choice for bipolar signals when high-event rate collider experiments are the target application.

One advantage of the deconvolution methods over the classical OF, is that the only information required is a good representation of the reference pulse shape, while the OF needs additional information about the covariance matrix for the current pileup level. Another advantage of deconvolution is the possibility to estimate the pileup signals amplitude.

The results obtained using a simplified toy Monte Carlo simulation gave some promising indications that for calorimeters operating at high occupancy level and when only a fraction of the pulse is acquired, the proposed SR method reduces the estimation error. Therefore, the proposed method is a good candidate for further investigation using full Monte Carlo simulation and real data from collider experiments operating at high luminosities. Nevertheless, when the channel occupancy is low, the OF method is the best choice, since it combines good performance with low computational cost.

The implemented algorithm for SR, using LP, can be considered as the classical approach. In this paper, we proposed a modification in this approach by the introduction of an asymmetry between the weights for positive and negative components of the objective function, in order to promote positive amplitude estimations. For future works, a deep investigation in modern SR theory is mandatory, focusing in computational cost minimization for online implementations.

References

[1] R. Wigmans, *Calorimetry: Energy Measurement in Particle Physics*, vol. 107. New York, NY, USA: Oxford Univ. Press, 2000.

[2] G. Bertuccio, E. Gatti, and M. Sapietro, "Sampling and optimum data processing of detector signals," *Nucl. Instrum. Methods Phys. Res. A, Accel. Spectrom. Detect. Assoc. Equip.*, vol. 322, no. 2, pp. 271–279, 1992.

[3] L. Evans and P. Bryant, "LHC machine," *J. Instrum.*, vol. 3, p. S08001, Aug. 2008.

[4] R. R. Wilson, "The Tevatron," Fermilab, Batavia, IL, USA, Tech. Rep. FERMILAB-TM-0763, 1978.

[5] W. E. Cleland and E. G. Stern, "Signal processing considerations for liquid ionization calorimeters in a high rate environment," *Nucl. Instrum. Methods Phys. Res. A, Accel. Spectrom. Detect. Assoc. Equip.*, vol. 338, nos. 2–3, pp. 467–497, 1994.

[6] H. Xu, D. Gong, and Y. Chiu, "A linear optimal filtering approach for pileup noise removal in high-rate liquid ionization calorimeters," in *Proc. IEEE Nucl. Sci. Symp. Med. Imag. Conf.*, Seoul, South Korea, Oct./Nov. 2013, pp. 1–6.

[7] P. Adzic *et al.*, "Reconstruction of the signal amplitude of the CMS electromagnetic calorimeter," *Eur. Phys. J. C-Particles Fields*, vol. C46, no. S1, pp. 26–35, Jul. 2006.

[8] L. M. de A. Filho, B. S. Peralva, J. M. de Seixas, and A. S. Cerqueira, "Calorimeter response deconvolution for energy estimation in high-luminosity conditions," *IEEE Trans. Nucl. Sci.*, vol. 62, no. 6, pp. 3265–3273, Dec. 2015.

[9] H. Muller *et al.*, "Front-end electronics for PWO-based PHOS calorimeter of ALICE," *Nucl. Instrum. Methods Phys. Res. A, Accel. Spectrom. Detect. Assoc. Equip.*, vol. 567, no. 1, pp. 264–267, 2006.

[10] K. Anderson, J. Pilcher, H. Sanders, and F. Tang, "Front-end electronics for the ATLAS tile calorimeter," in *Proc. 4th Workshop Electron. LHC Experim.*, 1998, pp. 1–7.

[11] A. Caldwell *et al.*, "Design and implementation of a high precision readout system for the ZEUS calorimeter," *Nucl. Instrum. Methods Phys. Res. A, Accel. Spectrom. Detect. Assoc. Equip.*, vol. 321, pp. 356–364, Sep. 1992.

[12] V. Abazov *et al.*, "The upgraded DØ detector," *Nucl. Instrum. Methods Phys. Res. A, Accel. Spectrom. Detect. Assoc. Equip.*, vol. 565, pp. 463–537, Sep. 2006.

[13] G. Aad *et al.*, "Readiness of the ATLAS liquid argon calorimeter for LHC collisions," *Eur. Phys. J. C*, vol. 70, no. 3, pp. 723–753, 2010.

[14] V. Radeka and S. Rescia, "Speed and noise limits in ionization chamber calorimeters," *Nucl. Instrum. Methods Phys. Res. A, Accel. Spectrom. Detect. Assoc. Equip.*, vol. 265, pp. 356–364, Mar. 1998.

[15] S. M. Kay, *Fundamentals of Statistical Signal Processing, Estimation Theory*. Englewood Cliffs, NJ, USA: Prentice-Hall, 1993.

[16] M. Elad, *Sparse and Redundant Representations. From Theory to Applications in Signal and Image Processing*. Springer, 2010.
[17] R. Gribonval and S. Lesage, "A survey of sparse component analysis for blind source separation: Principles, perspectives, and new challenges," in *Proc. 14th Eur. Symp. Artif. Neural Netw.*, 2006, pp. 323–330.
[18] A. Cichocki *et al.*, *Nonnegative Matrix and Tensor Factorizations*. Hoboken, NJ, USA: Wiley, 2009.
[19] R. A. DeVore and V. N. Temlyakov, "Some remarks on greedy algorithms," *Adv. Comput. Math.*, vol. 5, no. 1, pp. 173–187, 1995.
[20] I. F. Gorodnitsky and B. D. Rao, "Sparse signal reconstruction from limited data using FOCUSS: A re-weighted minimum norm algorithm," *IEEE Trans. Signal Process.*, vol. 45, no. 3, pp. 600–616, Mar. 1997.
[21] D. G. Luenberger and Y. Ye, *Linear and Nonlinear Programming*, 3rd ed. Springer, 2008.
[22] S. O. Haykin, *Adaptive Filter Theory*, 4th ed. Upper Saddle River, NJ, USA: Prentice-Hall, 2001.
[23] Y. Zhang, "Solving large-scale linear programs by interior-point methods under the MATLAB environment," Dept. Math. Statist., Univ. Maryland, Baltimore, MD, USA, Tech. Rep. TR96-01, 1995.
[24] S. Mehrotra, "On the implementation of a primal-dual interior point method," *SIAM J. Optim.*, vol. 2, no. 4, pp. 575–601, 1992.
[25] A. S. Nemirovski and M. J. Todd, "Interior-point methods for optimization," *Acta Numer.*, vol. 17, pp. 191–234, 2008.
[26] S. K. Mitra, *Digital Signal Processing: A Computer-Based Approach*, 3rd ed. New York, NY, USA: McGraw-Hill, 2005.
[27] W. R. Leo, *Techiniques for Nuclear and Particle Physics Experiments*, 2nd ed. Berlin, Germany: Springer-Verlag, 1994.
[28] J. Chapman, "ATLAS simulation computing performance and pile-up simulation in ATLAS," presented at the LPCC Detector Simulation Workshop, Geneva, Switzerland, 2011.
[29] S. Banerjee, "CMS simulation software," *J. Phys., Conf. Ser.*, vol. 396, no. 2, 2012, Art. no. 022003.
[30] P. J. Rousseeuw and K. Van Driessen, "A fast algorithm for the minimum covariance determinant estimator," *Technometrics*, vol. 41, no. 3, pp. 212–223, 1999.
[31] S. V. Chekanov, C. Levy, J. Proudfoot, and R. Yoshida, "New approach for jet-shape identification of TeV-scale particles at the LHC," *Phys. Rev. D, Part. Fields*, vol. 82, p. 094029, Nov. 2010.